Reducing the Overhead of OFDM Communications Over Underwater Acoustic Channels

Zhiqiang Liu
Acoustic Signal Processing and Systems
Naval Research Laboratory
Washington, DC 20375

T. C. Yang
Inst. of Applied Marine Physics and Undersea Technology
National Sun Yat-sen University
Kaohsiung 80424, Taiwan

ABSTRACT

In this paper, we propose a receiver design for single-input multiple-output (SIMO) orthogonal frequency division multiplexing (OFDM) communications over underwater acoustic (UWA) channels. The proposed design consists of two key components: i) time reversal based symbol detection that enables the use of short guard time intervals for inter-block interference avoidance; and ii) decision-directed channel tracking with error propagation control that eliminates the need of periodic training for channel tracking. The goal of our design is to improve bandwidth efficiency by reducing the amount of overhead typically associated with SIMO-OFDM UWA communications. The proposed design is tested at a sea-going experiment. The experimental results confirm the merits of our design and demonstrate considerable improvements over a competing alternative.

Categories and Subject Descriptors

H.4 [**Information Systems Applications**]: Miscellaneous

General Terms

Algorithms, Experimentation

Keywords

Underwater acoustic communications, time reversal, OFDM, error propagation

1. INTRODUCTION

In recent years, single-input multiple-output (SIMO) orthogonal frequency division multiplexing (OFDM) has gained attention as a promising means of supporting underwater acoustic communications (UWAC). Although SIMO-OFDM UWAC is intended to support high data rate, it is generally not bandwidth efficient due to its excessive use of overhead. In SIMO-OFDM, data symbols are transmitted in blocks separated by a zero guard interval known as zero postfix (ZP). To avoid inter-block interference (IBI), the ZP must be no shorter than channel delay spread. Since a UWA channel often has large delay spread, the use of long ZP thus constitutes the biggest source of overhead. Another source of overhead in SIMO-OFDM UWAC is the pilot or training symbols required for channel estimation. Since UWA channels are often long and also time varying, such overhead could be significant.

In this paper, we present a receiver design that improves bandwidth efficiency of SIMO-OFDM UWAC by requiring less amount of overhead. Our design is composed of two parts:

1. The first part of the design concerns the overhead caused by the use of long ZPs. Instead of using a large block size, we choose to reduce such overhead by employing time-reversal (TR) based SIMO-OFDM detection [4, 5, 3, 9, 8]. In TR-SIMO-OFDM detection, the TR operation combines multiple time-dispersive fading channels associated with SIMO-OFDM into a single one with generally smaller time dispersion and less fading. Our design focuses on how to reduce the ZP length as much as possible while meeting certain performance requirements.

2. The second part of the design concerns the overhead spent on channel estimation. To reduce such overhead, we employ decision-directed (DD) channel tracking where channel estimation is based on previous symbol decisions instead of training symbols. DD channel tracking is bandwidth efficient but its performance suffers from error propagation (EP) that occurs when some previous decisions are incorrect. To solve this problem, we incorporate error correcting (EC) and error detecting (ED) into channel tracking such that only correct decisions are used to update channel estimates.

The presented design was tested in a recent sea-going experiment. One major goal of this paper is to report our experimental results and compare our design with the state of the art.

The rest of this paper is organized as follows. In Section 2, we model the system. In Section 3, we describe receiver processing and explain how it helps reduce the overhead. In Section 4, we report the experimental results. Several concluding remarks are made in Section 5.

2. SYSTEM MODEL

Consider SIMO-OFDM UWAC with one transmitting element (TxE) and M receiving elements (RxEs). The overall

WUWNet'12, Nov. 5 - 6, 2012 Los Angeles, California, USA.

transmitted signal is the concatenation of a preamble signal and a data signal separated by a zero guard time interval larger than maximum possible channel delay spread. The preamble signal is used to acquire initial estimates of channel parameters required for symbol recovery. The data signal is a sequence of N zero-padded OFDM (ZP-OFDM) block signals, each containing one OFDM symbol followed by a ZP.

Let K be the number of subcarriers, L_{zp} the length of the ZP, and $b[i;k]$ the data symbol on the kth subcarrier in the ith block. The ith ZP-OFDM block signal can be written in discrete time as:

$$u(i;n) = \begin{cases} \sum b[i;k]e^{j\frac{2\pi}{K}kn} & 0 < n < K-1 \\ 0 & \text{else} \end{cases}. \quad (1)$$

Let B be the signal bandwidth and f_c the carrier frequency. The passband data signal is given by:

$$\tilde{u}(t) = \text{Re}\{e^{j2\pi f_c t} \sum_n \sum_i u(i; n-(i-1)P)\phi(t-n/B)\} \quad (2)$$

where $P = K + L_{zp}$ and $\phi(t) = \sin(\pi Bt)/(\pi Bt)$ is the sinc function. Among the K data symbols in each OFDM block, K_p are pilot symbols and the remaining $K_s = K - K_p$ are information-bearing symbols. Taking this into account, the bandwidth efficiency of the data signal can be expressed as:

$$\eta_{bw} = \frac{1 - K_p/K}{1 + L_{zp}/K} \quad \text{symbol/second/Hz.} \quad (3)$$

A major goal we are about to pursue in this work is to improve η_{bw} by coming up with a receiver design that supports the use of small L_{zp} and K_p for given K.

Assume a linear time-varying (LTV) multipath channel between the TxE and the mth RxE and model its impulse response as:

$$c_m(t;\tau) = \sum_\mu A_{m,\mu}(t)\delta(\tau - \tau_{m,\mu}(t)) \quad (4)$$

where $A_{m,\mu}(t)$ and $\tau_{m,\mu}(t)$ denote the time-varying path amplitude and delay of the μth path. Under this channel model, the passband received data signal at the mth RxE can be written as

$$\tilde{y}_m(t) = \sum_\mu A_{m,\mu}[i]\tilde{u}(t - \tau_{m,\mu}(t)) + \text{noise}. \quad (5)$$

For a multipath channel, the difference between the largest and the smallest path delays is often called channel delay spread. An upper bound of channel delay spread, denoted by τ_{max}, is assumed known in our design.

3. RECEIVER PROCESSING

In this section, we describe receiver processing used to recover data symbols from the M received signals. For development of receiver processing algorithms, it is assumed that:

A1) All path delays experience similar Doppler scaling within each ZP-OFDM block such that

$$\tau_{m,\mu}(t) = \tau_{m,\mu}[i] - \alpha_m[i]t, \quad t \in \mathcal{D}_i, \quad i = 1, \ldots, N,$$

where $a_m[i]$'s are called Doppler scaling factors (DSFs) and $\mathcal{D}_i$ stands for the time interval occupied by the ith ZP-OFDM block signal.

A2) The path amplitudes $A_{m,\mu}(t)$ remain constant within the interval $\mathcal{D}_i$ such that

$$A_{m,\mu}(t) = A_{m,u}[i], \quad t \in \mathcal{D}_i.$$

A3) The channel parameters $A_{m,\mu}[i]$, $\tau_{m,\mu}[i]$, $\alpha_m[i]$ vary slowly during the whole transmission.

Readers are referred to [7, 11] for a brief justification of these assumptions in undersea environments. In addition, it is assumed that an initial estimate of those channel parameters have already been made available via preamble based parameter estimation.

3.1 DSF Compensation

The effects of DSFs can be largely compensated via resampling [11]. Under assumption A1)-A3), it can be shown that DSF compensation transforms an LTV channel into a block-wise linear time invariant (LTI) channel. Consequently, the resultant samples at the mth RxE can be written as:

$$z_m[n] = \sum_{i=1}^{N} x_m[i; n-(i-1)P] + \text{noise} \quad (6)$$

where

$$x_m[i;n] = e^{j\theta[i]}u[i;n] \star h_m[i;n] \quad (7)$$

with $\star$ denoting linear convolution and

$$h_m[i;n] = \sum_\mu A_{m,\mu}[i]e^{-2\pi f_c \tau_{m,\mu}[i]}\phi(n/B - \tau_{m,\mu}[i]) \quad (8)$$

representing the impulse response of the block-wise LTI channel of a maximum possible order $L_h = \lceil \tau_{max}B \rceil$. Note that in writing (6), we have assumed $\alpha_m[i] \approx \hat{\alpha}_m[0]$ with $\alpha_m[0]$ standing for an initial estimate of DSF. To account for small DSF errors $\alpha_m[i] - \hat{\alpha}_m[0]$, a block-dependent constant phase term $e^{j\theta[i]}$ is introduced in (7). This constant phase $\theta[i]$ will be estimated and compensated by inserting K_p pilot symbols in each data block. For notational simplicity, we absorb the phase term $e^{j\theta[i]}$ into $u[i;n]$ in our ensuring discussions. In (8), the block index i is introduced to account for possible variations of $h_m[i;n]$ from one block to another. This is necessary because even a small variation of $\tau_{m,\mu}[i]$ could induce a significant change to $h_m[i;n]$ due to the multiplying factor f_c in (8).

Eq. (6) constitutes a data model for SIMO ZP-OFDM transmissions over block-wise LTI channels. With the goal of improving bandwidth efficiency, we consider recovering data symbols via TR-SIMO-OFDM detection [4, 5, 3, 9, 8]. In TR-SIMO-OFDM detection, the TR operation converts multiple time-dispersive fading channels in SIMO-OFDM into a single channel with generally smaller time dispersion and less fading. It thus becomes possible for us to use small L_{zp} without sacrificing detection performance, even when the original channels have large delay spread. As a byproduct, TR-SIMO-OFDM detection also helps lower receiver complexity by reducing the number of required OFDM demodulators to one. To motivate TR-SIMO-OFDM, we first describe the state of the art detection scheme [7, 6], and point out its pros and cons. Because this scheme relies on the use of maximum ratio combining (MRC), it is referred to as MRC-SIMO-OFDM detection for convenience.

3.2 MRC-SIMO-OFDM Detection

In MRC-SIMO-OFDM detection, data blocks $\mathbf{b}[i] = [b[i;0], \ldots, b[i;K-1]]^T$ are detected independently in a block by block fashion. To avoid possible IBI in (6), $L_{zp} \geq L_h$ is used. Two successive operations are involved in detecting each data block. First, ZP-OFDM demodulation is performed to remove inter-carrier interference (ICI) and produce M intermediate decision statistics for each data block. Then, MRC is taken to combine those intermediate decision statistics into a final one. To acquire channel knowledge required by MRC, MRC-SIMO-OFDM detection relies on insertion of pilot symbols in each data block. Because the channels are of order L_h, $K_p > L_h$ is generally required unless one exploits sparsity of channel responses by using, e.g., compressed sensing [2].

As demonstrated in several sea-going experiments [7, 6], MRC-SIMO-OFDM detection has been shown capable of offering robust performance in various undersea environments. On the other hand, since $L_{zp} \geq L_h$ and $K_p > L_h$ are used, η_{bw} in (3) is at most $(1-L_h/K)/(1+L_h/K)$. For UWA channels, L_h could be tens or hundreds due to large channel delay spread. To reduce L_h/K and therefore improve η_{bw}, one obvious approach is to design $K \gg L_h$. Unfortunately, this approach could be infeasible, because i) the value of K is limited by channel coherence time that could be small in UWA channel environments, ii) a large K reduces subcarrier spacing and therefore, demands high-resolution frequency offset estimation that could be difficult in UWA channels, iii) a large K requires high computational complexity that might not be affordable especially for real-time implementation, and iv) a too large K could even lead to system breakdown as observed in [12]. For these reasons, MRC-SIMO-OFDM detection might not offer desirable bandwidth efficiency. For example, $L_{zp} = 300$ and $K = 1024$ were recommended in [7] for at-sea tests. This results in $\eta_{bw} < 54\%$ which is fairly low for high-rate applications.

3.3 TR-SIMO-OFDM detection

Just like MRC-SIMO-OFDM detection, TR-SIMO-OFDM detection involves multichannel combining and ZP-OFDM demodulation but in a *reverse* order. To detect a data block, say, $\mathbf{b}[j]$, TR is first performed on $z_m[n]$ to form $z[n] = \sum_{m=1}^{M} z_m^{(d)}[n] \star \hat{h}_m^*[j; \frac{L_{zp}}{2} - n]$ where $\hat{h}_m[j;n]$ denotes an estimate of $h_m[j;n]$. Using (6) and (7), $z[n]$ can be expressed as:

$$z[n] = \sum_{i=1}^{N} x^{(j)}[i; n-(i-1)P] + \text{noise} \tag{9}$$

where $x^{(j)}[i;n] = u[i;n] \star q^{(j)}[i;n]$ and

$$q^{(j)}[i;n] = \sum_{m=1}^{M} h_m[i;n] \star \hat{h}_m^*[j; \frac{L_{zp}}{2} - n]. \tag{10}$$

The relationship of (9) suggests that the TR operation has rendered SIMO ZP-OFDM transmissions into single-input single-output (SISO) ZP-OFDM transmissions over a block-wise LTI channel $q^{(j)}[i;n]$ that is referred to as TR channel.

After the TR operation, ZP-OFDM demodulation is then performed on block $\mathbf{z}[j] := [z[jP], \ldots, z[jP+P-1]]^T$ to recover $\mathbf{b}[j]$. For reduced computational complexity, such demodulation is implemented via FFT as:

$$\mathbf{d}[j] = \mathbf{F}_K \mathbf{R}_{ola} \mathbf{z}[j] \tag{11}$$

where the $K \times K$ matrix $\mathbf{F}_K$ denotes the K-point FFT, and the $K \times P$ matrix $\mathbf{R}_{ola}$ represents the overlap-add (OLA) operation that converts ZP-OFDM into CP-OFDM.

Targeting at highest possible bandwidth efficiency, we would like to reduce L_{zp} as much as possible while still meeting certain performance requirements. At high input signal-to-noise ratios (SNRs) – typical for UWAC, performance of TR-SIMO-OFDM detection can be measured by the signal-to-interference ratio (SIR) $\rho_{SIR}^{(j)}$ of $\mathbf{d}[j]$ which, under assumption A3), can be well approximated by:

$$\rho_{SIR}^{(j)} = \frac{\sum_{n=0}^{L_{zp}} |q^{(j)}[j;n]|^2}{\sum_{n \geq L_{zp}+1} |q^{(j)}[j;n]|^2 + \sum_{n<0} |q^{(j)}[j;n]|^2}. \tag{12}$$

If the ultimate goal is to avoid the IBI completely, i.e., $\rho_{SIR}^{(j)} = \infty$, then $L_{zp} > 2L_h$ should be chosen at the expense of bandwidth efficiency. In practice, achieving zero IBI at all expenses (especially, at the expense of bandwidth efficiency loss) is seldom a good idea, and it often makes little (if any) difference in terms of coded performance, thanks to the use of error-correcting coding. A more reasonable system design often targets at meeting certain performance requirements, while improving bandwidth efficiency as much as possible. With this in mind, it thus makes sense to design L_{zp} as small as possible so long as the corresponding $\rho_{SIR}^{(j)} > \rho_0$ for some threshold ρ_0 determined by performance specifications.

The SIR in (12) represents the percentage of the power of the TR channel lying within the ZP interval. Thanks to the TR operation, as proved in [10], the TR channel is impulse-like with most of its energy concentrated within a small interval around $n = L_{zp}/2$. This suggests that TR-SIMO-OFDM detection supports the use of $L_{zp} \ll L_h$ without causing much (if any) IBI. How to minimize L_{zp} under the constraint $\rho_{SIR}^{(j)} > \rho_0$ has been addressed in [10]. One example in [10] has shown that in a typical shallow water environment, TR-SIMO-OFDM detection is capable of reducing the ZP length by six times with $M = 16$ receiving elements.

3.4 DD Channel Tracking with EP Control

Both TR and ZP-OFDM demodulation require up-to-date channel estimates. While conventional pilot-based channel estimation performs well, it comes at the expense of bandwidth efficiency loss especially in the case of UWA channels. One reason is that a UWA channel typically requires a large number of pilot symbols to estimate because of its long impulse response. Another reason is that a UWA channel tends to vary with time, and therefore, its estimate must be updated frequently. For improved bandwidth efficiency, we focus in this work on DD channel tracking that does not require the use of pilot symbols. In DD channel tracking, data detection and channel estimation alternate. A data block is first detected based on channel estimates in the previous block. Once detected, the data block is then treated as pilot symbols to update channel estimates for the next block. As in any DD approaches, DD channel tracking suffers from error propagation that occurs when channel updates are based on an incorrectly detected data block.

To prevent error propagation, we add two successive steps to DD channel tracking, namely, error correcting (EC) and error detecting (ED). EC is applied to correct possible errors in a detected data block, and ED is used to determine if the detected data block after error correction is correct or not. If

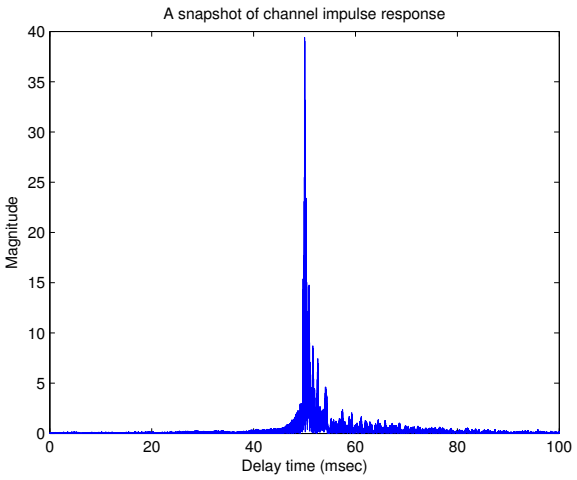

Figure 1: A snapshot of the channel impulse response at the first receiving hydrophone, obtained by using the LFM signal.

correct, the channels are re-estimated using the data block. Otherwise, the channel estimates remain unchanged. In this way, we are able to ensure that all channel updates are based on correct data blocks. In modern digital communication networks, EC is done at the physical layer by using channel coding, and ED is usually performed at the data link layer by checking the CRC (cyclic redundancy check). Therefore, the proposed channel tracking scheme requires a cross-layer system design. If a cross-layer design is impossible, one can rely on insertion of a small number of pilot symbols in each data block to facilitate ED.

4. PERFORMANCE RESULTS WITH EXPERIMENTAL DATA

4.1 Experiment Setting

The experiment was conducted at sea near Kaohsiung, Taiwan on May 11, 2011. The signal described in Section 2 was transmitted repeatedly from a transducer at a depth of about 5 m. To avoid interference, a guard time of 300 msec was used between two repetitions. The transmitted signal was received by a vertical vector sensor array of six hydrophones ($M = 6$) that is 2.5 km away. The six receiving hydrophones were equally spaced by 1 m with the first (deepest) one submerged at a depth of about 11 m. The transducer was mounted at the rear end of one anchored ship and the receiving sensor array was moored to the ocean bottom.

To generate information symbols, random information bits are first encoded by a rate-1/2 convolutional encoder with generator polynomial $[65, 57]$. The code is chosen arbitrarily and can be replaced by more bandwidth-efficient codes, if so desired. The encoded bits are then interleaved by a block interleaver of depth 8 prior to quadrature phase shift keying (QPSK) modulation. The peak-to-average power ratio (PAR) is controlled by using selected mapping [1]. The training and pilot symbols are generated from an arbitrary binary pseudo-random sequence by using binary phrase shift keying (BPSK) modulation.

The signaling parameters used are $f_c = 18560$ Hz and $K = 512$. Each data OFDM block includes $K_p = 16$ pilot tones that are equally spaced in the frequency domain. The pilot tones are used for correcting a constant phase offset across subcarriers, and do not serve other purposes such as DD channel estimation. Three cases of the ZP length are implemented: i) $L_{zp} = 300$ or $T_{zp} = 60$ msec, ii) $L_{zp} = 100$ or $T_{zp} = 20$ msec, and iii) $L_{zp} = 50$ or $T_{zp} = 10$ msec. The (data part) bandwidth efficiencies for the three cases are $\eta_{bw}^{(d)} = 61\%, 86\%, 94\%$, respectively.

To probe the channel, a linearly frequency modulated (LFM) signal was sent at the beginning. The LFM signal is well separated from the transmitted signal to avoid any possible interference. By matched filtering the received signal with the LFM signal, Fig. 1 plots a snapshot of the channel impulse response at the first receiving hydrophone. From the snapshot, it can be implied that the IBI should be negligible with $L_{zp} = 300$, fairly small with $L_{zp} = 100$ and relatively strong with $L_{zp} = 50$. For this reason, we hereafter call the three cases as IBI-free, IBI-small, and IBI-strong cases.

4.2 BER Performance Comparison

By processing the same set of recorded data, we compare TR-SIMO-OFDM with MRC-SIMO-OFDM in terms of their coded and uncoded performance measured by the bit error rate (BER) within each data block. In both schemes, DD channel tracking with EP control is applied, with the initial channel estimates obtained from preamble-based parameter estimation. Because the two schemes perform identically in the IBI-free case, only the IBI-small and IBI-strong cases are presented.

Figs. 2(a) and 2(b) compare the two schemes for the IBI-small case (i.e., $L_{zp} = 100$). In this case, TR-SIMO-OFDM achieves marginally better uncoded performance but the same perfect coded performance. This is no surprise because the IBI is not much a factor when $L_{zp} = 100$. This, to certain extent, confirms our claim that TR-SIMO-OFDM is capable of achieving the same optimal performance as MRC-SIMO-OFDM. The comparison is repeated for the IBI-strong case (i.e., $L_{zp} = 50$) in Figs. 3(a) and 3(b) which reveal that TR-SIMO-OFDM is much more robust against the increased IBI. Fig. 4 plots the the SIR ratio defined in (12) for the IBI-strong case. The results again confirm that TR-SIMO-OFDM experiences much less IBI as compared to MRC-SIMO-OFDM. In addition, the level of IBI in the case of TR-SIMO-OFDM appears less fluctuating. This explains why TR-SIMO-OFDM experiences less performance outages as evident in Figs. 3(a) and 3(b).

4.3 Effects of EP Control

One unique feature of the proposed DD channel tracking scheme is its capability of preventing EP. To investigate how the EP control improves the performance, we examine the performance of TR-SIMO-OFDM when $M = 2$ and $L_{zp} = 50$. The proposed EP control scheme consists of two components: EC and ED. Each component could be either included or excluded in EP control. Fig. 5 shows the BER performance for two scenarios: i) No EP control, and ii) complete EP control with both EC and ED. The results indicate that i) error propagation happens in all cases but to different extents; ii) significant performance improvement is achieved with both EC and ED. These results validate our design.

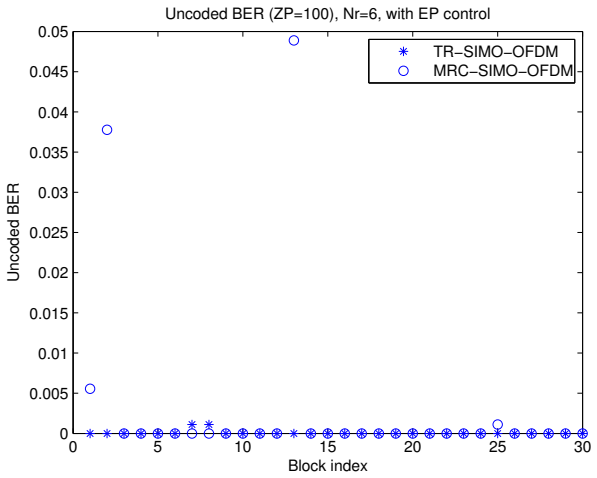

(a) Uncoded BER

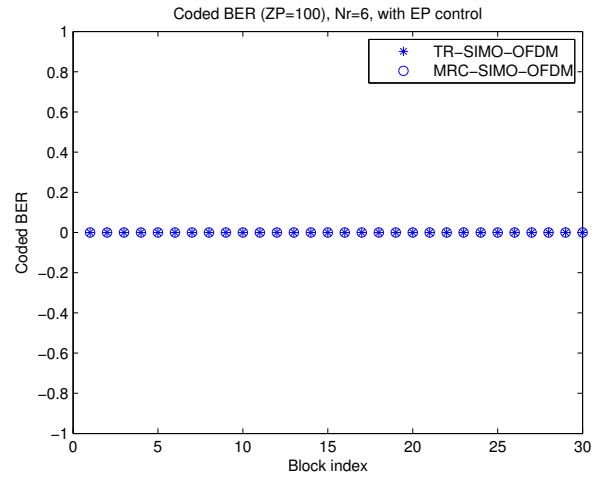

(b) Coded BER

Figure 2: BER performance comparison with $L_{zp} = 100$ and $M = 6$

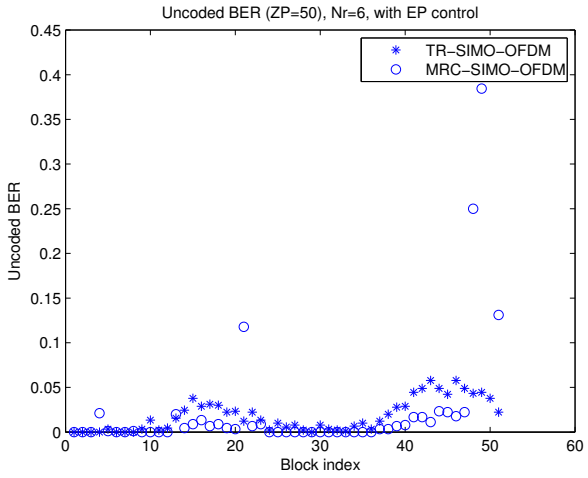

(a) Uncoded BER

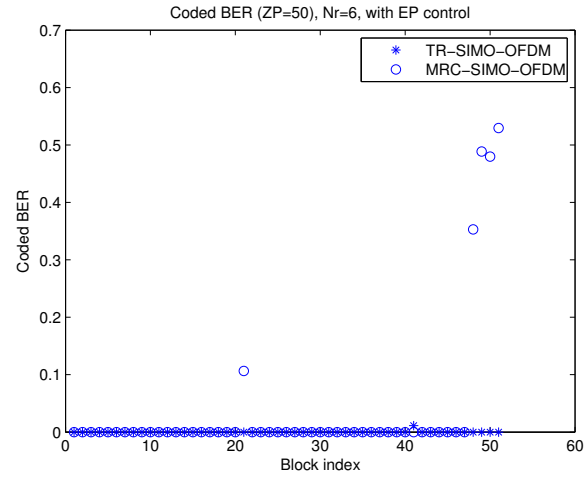

(b) Coded BER

Figure 3: BER performance comparison with $L_{zp} = 50$ and $M = 6$

5. CONCLUSION

In this paper, we presented a receiver design for bandwidth efficient SIMO-OFDM communications over UWA channels. By reducing the amount of overhead at no performance loss, our design was capable of improving the tradeoffs among bandwidth efficiency, error performance and complexity. The merits of our design were confirmed by an at-sea experiment. Our design appears well suitable for real-time implementation. As a future research direction, we will focus on implementation issues of this design.

6. ACKNOWLEDGMENTS

This work is supported by Office of Naval Research. The experiment was supported by the Taiwan National Science Council. The authors would like to thank all participants of the sea-going experiment for their assistance.

7. REFERENCES

[1] R. Bauml, R. Fischer, and J. Huber. Reducing the

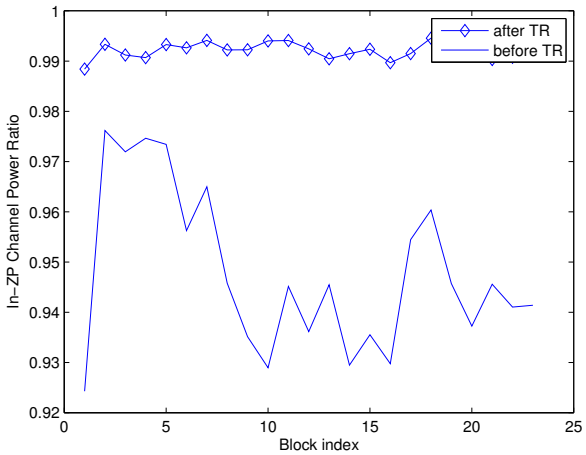

Figure 4: The SIR ratio

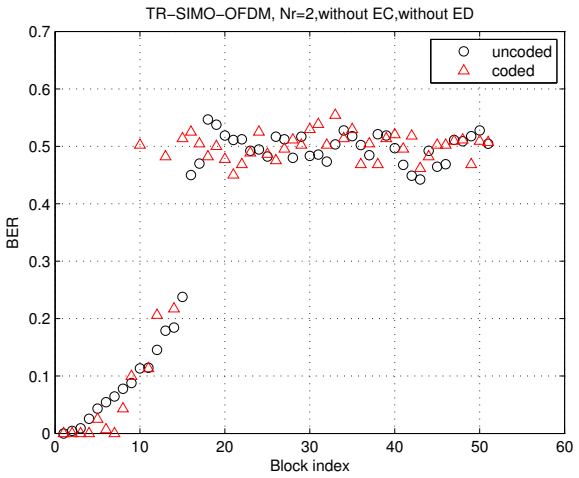

(a) No EP Control

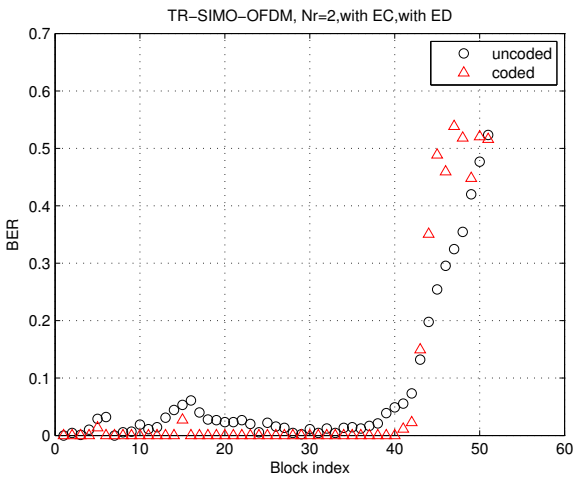

(b) Complete EP

Figure 5: Effects of error propagation control ($M = 4$, $L_{zp} = 50$)

peak-to-average power ratio of multicarrier modulation by selected mapping. *Electronics Letters*, 32(22):2056–2057, 1996.

[2] C. Berger, S. Zhou, J. Preisig, and P. Willett. Sparse channel estimation for multicarrier underwater acoustic communication: From subspace methods to compressed sensing. *IEEE Transactions on Signal Processing*, 58(3):1708–1721, 2010.

[3] J. Gomes, C. Berger, and S. Jesus. Demodulation of underwater OFDM transmissions by time reversal and basis pursuit methods. In *Proc. of European Wireless Conf.*, pages 506–514, 2011.

[4] J. Gomes, A. Silva, and S. Jesus. Experimental assessment of time-reversed OFDM underwater communications. *Journal of the Acoustical Society of America*, 123(5):3891–3891, 2008.

[5] J. Gomes, A. Silva, and S. Jesus. OFDM demodulation in underwater time-reversed shortened channels. In *OCEANS*, pages 1 –8, Sep. 2008.

[6] B. Li, S. Zhou, M. Stojanovic, and L. Freitag. Pilot-tone based ZP-OFDM demodulation for an underwater acoustic channel. In *OCEANS 2006*, pages 1–5, 2006.

[7] B. Li, S. Zhou, M. Stojanovic, L. Freitag, and P. Willett. Multicarrier communication over underwater acoustic channels with nonuniform Doppler shifts. *IEEE Journal of Oceanic Engineering*, 33(2):198–209, 2008.

[8] C. Lini, W. Zhang, J. Yoon, and J. Park. Intercarrier interference cancellation for time reversed OFDM systems. In *Proc. of Symposium on Ultrasonic Electronics*, pages 415–416, 2010.

[9] X. Liu, B. Wang, G. Zeng, G. Ge, and S. Ding. Time reversal based channel self-adaptive OFDM in complex environment. In *Proc. of Microwave and Millimeter Wave Technolgy Conf.*, pages 1633–1636, 2010.

[10] Z. Liu and T. Yang. On the design of cyclic prefix length for time-reversed OFDM. *IEEE Transactions on Wireless Communications*, 2012. accepted; downloadable at https://sites.google.com/site/zliuee/.

[11] S. Mason, C. Berger, S. Zhou, and P. Willett. Detection, synchronization, and Doppler scale estimation with multicarrier waveforms in underwater acoustic communication. *IEEE Journal on Selected Areas in Communications*, 26(9):1638–1649, 2008.

[12] M. Stojanovic. Low complexity OFDM detector for underwater acoustic channels. In *OCEANS 2006*, pages 1–6, 2006.